


# Broadband enhancement of on-chip single-photon extraction via tilted hyperbolic metamaterials

Cite as: Appl. Phys. Rev. **7**, 021403 (2020); <https://doi.org/10.1063/1.5141275>

Submitted: 04 December 2019 . Accepted: 24 March 2020 . Published Online: 05 May 2020

Lian Shen, Xiao Lin , Mikhail Y. Shalaginov , Tony Low, Xianmin Zhang, Baile Zhang, and Hongsheng Chen

## COLLECTIONS

 This paper was selected as Featured



View Online



Export Citation



CrossMark

## ARTICLES YOU MAY BE INTERESTED IN

[Identification of light sources using machine learning](#)

Applied Physics Reviews **7**, 021404 (2020); <https://doi.org/10.1063/1.5133846>

[Diffused morphotropic phase boundary in relaxor-PbTiO<sub>3</sub> crystals: High piezoelectricity with improved thermal stability](#)

Applied Physics Reviews **7**, 021405 (2020); <https://doi.org/10.1063/5.0004324>

[Genesis and evolution of extended defects: The role of evolving interface instabilities in cubic SiC](#)

Applied Physics Reviews **7**, 021402 (2020); <https://doi.org/10.1063/1.5132300>



AVS Quantum Science

SPECIAL ISSUE:  
Quantum Sensing and Metrology

SUBMIT TODAY!

Co-Published by



# Broadband enhancement of on-chip single-photon extraction via tilted hyperbolic metamaterials

Cite as: Appl. Phys. Rev. **7**, 021403 (2020); doi: [10.1063/1.5141275](https://doi.org/10.1063/1.5141275)

Submitted: 4 December 2019 · Accepted: 24 March 2020 ·

Published Online: 5 May 2020



View Online



Export Citation



CrossMark

Lian Shen,<sup>1,2,3</sup> Xiao Lin,<sup>1,4,a)</sup>  Mikhail Y. Shalaginov,<sup>5</sup>  Tony Low,<sup>6</sup> Xianmin Zhang,<sup>1,2,3</sup> Baile Zhang,<sup>4,7,a)</sup> and Hongsheng Chen<sup>1,2,a)</sup>

## AFFILIATIONS

<sup>1</sup>Interdisciplinary Center for Quantum Information, State Key Laboratory of Modern Optical Instrumentation, College of Information Science and Electronic Engineering, Zhejiang University, Hangzhou 310027, China

<sup>2</sup>ZJU-Hangzhou Global Science and Technology Innovation Center, Key Lab. of Advanced Micro/Nano Electronic Devices & Smart Systems of Zhejiang, Zhejiang University, Hangzhou 310027, China

<sup>3</sup>Ningbo Research Institute, Zhejiang University, Ningbo 315100, China

<sup>4</sup>Division of Physics and Applied Physics, School of Physical and Mathematical Sciences, Nanyang Technological University, Singapore 637371, Singapore

<sup>5</sup>Department of Materials Science and Engineering, Massachusetts Institute of Technology, 77 Massachusetts Avenue, Cambridge, Massachusetts 02139, USA

<sup>6</sup>Department of Electrical and Computer Engineering, University of Minnesota, Minneapolis, Minnesota 55455, USA

<sup>7</sup>Centre for Disruptive Photonic Technologies (CDPT), School of Physical and Mathematical Sciences, Nanyang Technological University, Singapore 637371, Singapore

<sup>a)</sup>Authors to whom correspondence should be addressed: [xiaolinbnwj@ntu.edu.sg](mailto:xiaolinbnwj@ntu.edu.sg); [blzhang@ntu.edu.sg](mailto:blzhang@ntu.edu.sg); and [hansomchen@zju.edu.cn](mailto:hansomchen@zju.edu.cn)

## ABSTRACT

On-chip single-photon sources with high repetition rates are a fundamental block for quantum photonics and can enable applications such as high-speed quantum communication or quantum information processing. Ideally, such single-photon sources require a large on-chip photon extraction decay rate, especially over a broad spectral range, but this goal has remained elusive so far. Current approaches implemented to enhance the spontaneous emission rate include photonic crystals, optical cavities, metallic nanowires, and metamaterials. These approaches either have a strong reliance on the frequency resonance mechanisms, which unavoidably suffer from the issue of narrow working bandwidth, or are limited by poor outcoupling efficiency. Here, we propose a feasible scheme to enhance the on-chip photon extraction decay rate of quantum emitters through the tilting of the optical axis of hyperbolic metamaterials with respect to the end-facet of nanofibers. The revealed scheme is applicable to arbitrarily orientated quantum emitters over a broad spectral range extending up to  $\sim 80$  nm for visible light. This finding relies on the emerging unique feature of hyperbolic metamaterials if their optical axis is judiciously tilted. Hence, their supported high- $k$  (i.e., wavevector) hyperbolic eigenmodes, which are intrinsically confined inside them if their optical axis is un-tilted, can now become momentum-matched with the guided modes of nanofibers, and more importantly, they can efficiently couple into nanofibers almost *without reflection*.

Published under license by AIP Publishing. <https://doi.org/10.1063/1.5141275>

The on-chip source of single photons is of extreme importance for the exploration and development of integrated quantum information technology, including quantum cryptography,<sup>1</sup> quantum computation,<sup>2,3</sup> and quantum communication,<sup>4–6</sup> since existing quantum networks transmit information through single photons. One of the key characteristics of on-chip single-photon sources is the repetition rate.<sup>7</sup> This is because a higher repetition rate allows higher bit rates in

quantum communication and faster readout of stationary qubits.<sup>8–11</sup> To be specific, the repetition rate is determined by the photon extraction decay rate of quantum emitters into nanofibers, which is equal to the product of emitter's spontaneous emission rate and the coupling efficiency of excited photons into nanofibers or waveguides. As such, it is highly desirable to enhance the on-chip photon extraction decay rate for single-photon sources, especially over a broad spectral range.

There are extensive approaches to enhancing the spontaneous emission rate by using, for example, photonic crystals, optical cavities, metallic nanowires, and metamaterials.<sup>12–29</sup> However, these approaches either have a strong reliance on the frequency resonance mechanism, which unavoidably suffers from the issue of narrow working bandwidth or are limited by the poor outcoupling efficiency. Recently, the photonic hypercrystals, which combine the large broadband photonic density-of-states provided by hyperbolic metamaterials with the high light-scattering efficiency of photonic crystals, are reported to be a promising platform for the enhancement of photon extraction decay rate into *free space* over a broad visible spectral range (e.g., 580–700 nm).<sup>30</sup> However, the realization of large *on-chip* photon extraction decay rates over a broad spectral range still remains an open challenge.

To be specific, only a few proposals have been put forward to enhance the on-chip photon extraction decay rate by using, for example, tapered nanofibers, metallic structures that support gap surface plasmons integrated with phase-matched nanofibers, and hyperbolic metamaterials.<sup>21–37</sup> These proposals either have a weak enhancement of the photon extraction decay rate or can work only at a narrow frequency range,<sup>21–37</sup> due to the low spontaneous emission rate,<sup>21–26</sup> the poor outcoupling efficiency,<sup>29–36</sup> or the phase matching condition between the excited gap surface plasmons and the guidance modes of nanofibers.<sup>27,28</sup> To clearly illustrate this issue, those proposals based on hyperbolic metamaterials are briefly analyzed as a typical example below. For hyperbolic metamaterials, placing a quantum emitter in their vicinity generally provides a drastic enhancement of the spontaneous emission rate over a broad spectral range, due to their broadband large photonic density-of-states.<sup>37–43</sup> However, their large photonic density-of-states cannot directly lead to a high photon extraction decay rate, due to the low coupling efficiency, which originates from the fact that the supported high- $k$  (i.e., wavevector) eigenmodes generally cannot propagate to the far field but are intrinsically confined inside the hyperbolic metamaterials.<sup>37–43</sup> As such, the hyperbolic metamaterials, including metal-dielectric multilayered structures<sup>29</sup> and those that are nanopatterned or adiabatically tapered,<sup>31–33</sup> are thought to be less practical to achieve the broadband enhancement of on-chip photon extraction decay rates.

Here, we introduce a feasible scheme where the above intrinsic limitations in hyperbolic metamaterials can be overcome, thus enabling a flexible enhancement of the on-chip photon extraction decay rate over a broad spectral range. To be specific, such a capability is enabled by the judicious tilting of the optical axis of hyperbolic metamaterials with respect to the end-facet of nanofibers; see the structural schematic in Fig. 1(a). Due to the tilted optical axis, the high- $k$  eigenmodes in the hyperbolic metamaterials can become momentum-matched with the guided modes in nanofibers, and more importantly, their reflection would be suppressed at the interface between hyperbolic metamaterials and nanofibers. In other words, the high- $k$  eigenmodes can now safely couple into nanofibers. This way, the tilted hyperbolic metamaterials here are distinctly different from un-tilted hyperbolic metamaterials,<sup>29–33</sup> and they become practical for the broadband enhancement of on-chip single-photon extraction. We highlight that due to the advancement of nanotechnology, it is now feasible to implement tilted hyperbolic metamaterials in experiments.<sup>44–47</sup> Another advantage is that the proposed

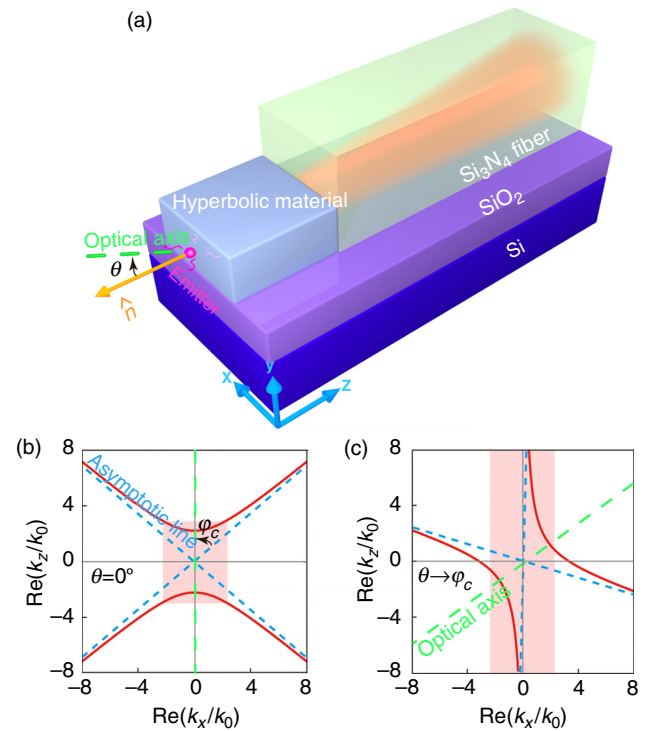


**FIG. 1.** Schematic of enhancing the on-chip single-photon extraction decay rate via tilted hyperbolic metamaterials. (a) Structural setup. A quantum emitter, modeled by a dipole, is positioned very close to a hyperbolic metamaterial, which is integrated with a nanofiber and whose optical axis is tilted by an angle of  $\theta$  with respect to the normal vector  $\hat{n} = -\hat{z}$  of the interface. The fabrication of the proposed structure in Fig. 1(a) should be feasible in experiments and compatible with current planar technology by following, for example, the technique discussed in this paper (see, for example, Figs. S2 and S3) and the technique for the fabrication of tilted hyperbolic metamaterials developed recently in Refs. 44–47. (b, c) Isofrequency contour of transparent hyperbolic metamaterials with (b)  $\theta = 0$  and (c)  $\theta \rightarrow \varphi_c$ , where  $\varphi_c$  is the angle between the optical axis and the asymptotic line of hyperbolic isofrequency contours. The colored or shaded region in (b, c) has  $|\text{Re}(k_x/k_0)| \leq n_{\text{Si}_3\text{N}_4}$ ; the excited hyperbolic modes inside this region in (c) are able to efficiently couple into the nanofiber almost without reflection.

scheme is applicable for quantum emitters with arbitrary orientation. Our work thus represents a vital step toward the implementation of spectrally broad single-photon sources with high repetition rates for on-chip quantum networks.

We start with the analysis of the corresponding underlying mechanism from the perspective of the isofrequency contour of eigenmodes in hyperbolic metamaterials. For the hyperbolic metamaterial, its optical axis has an angle  $\theta$  with respect to the normal vector  $\hat{n}$  ( $\hat{n} \parallel \hat{z}$ ) of the end-facet (parallel to the  $x$ - $y$  plane) of nanofibers [Fig. 1(a)]. The fabrication of the proposed structure in Fig. 1(a) should be feasible in experiments and compatible with current planar technology by following, for example, the technique discussed in Figs. S2–S3 (see the [supplementary material](#)) and the technique for the fabrication of tilted hyperbolic metamaterials developed recently in Refs. 44–47. The hyperbolic metamaterial has a relative permittivity of  $[\epsilon_{\parallel}, \epsilon_{\parallel}, \epsilon_{\perp}]$ , where  $\epsilon_{\parallel}$  and  $\epsilon_{\perp}$  are the components parallel and perpendicular to the

optical axis, respectively. This way, the isofrequency contour in the  $x$ - $z$  plane can be described by

$$\begin{aligned} & (\varepsilon_{\parallel} \sin^2 \theta + \varepsilon_{\perp} \cos^2 \theta) k_z^2 + 2(\varepsilon_{\parallel} - \varepsilon_{\perp}) \sin \theta \cos \theta k_x k_z \\ & + (\varepsilon_{\parallel} \cos^2 \theta + \varepsilon_{\perp} \sin^2 \theta) k_x^2 = k_0^2 \varepsilon_{\parallel} \varepsilon_{\perp}, \end{aligned} \quad (1)$$

where  $k_x$  and  $k_z$  are the components of wavevector  $\bar{k}$ , parallel and perpendicular to the end-facet of nanofibers [Fig. 1(a)], respectively;  $k = |\bar{k}| = \sqrt{k_x^2 + k_z^2}$ ;  $k_0 = \omega/c$ ; and  $c$  is the light speed in free space. Below, we set  $\text{Re}(\varepsilon_{\parallel}) > 0$  and  $\text{Re}(\varepsilon_{\perp}) < 0$ .

We emphasized that the term related to  $k_z^2$  in Eq. (1) disappears if  $\varepsilon_{\parallel} \sin^2 \theta + \varepsilon_{\perp} \cos^2 \theta = 0$  or  $\theta = \varphi_c$ , where  $\varphi_c = \tan^{-1}(\sqrt{-\varepsilon_{\perp}/\varepsilon_{\parallel}})$  is the critical angle between the optical axis and the asymptotic line of hyperbolic isofrequency contours [Fig. 1(b)]. As a result, there is always only the unique solution of  $k_z$  for an arbitrary value of  $k_x$  in Eq. (1) if  $\theta = \varphi_c$  [Fig. 1(c)]. In contrast, there is always two solutions of  $k_z$  for an arbitrary value of  $k_x$  if  $\theta = 0$  [Fig. 1(b)].

The unique feature of hyperbolic isofrequency contour in Fig. 1(c) can lead to two prominent ways to enhance the on-chip photon extraction decay rate in Fig. 1(a). First, the supported high- $k$  (i.e.,  $k \gg k_0$ ) hyperbolic modes become to have a small value of  $k_x$  if  $\theta = \varphi_c$ . To be specific, we have  $|\text{Re}(k_x/k_0)| \leq n_{\text{fiber}}$  even if  $k \rightarrow \infty$  in the colored region in Fig. 1(c), where  $n_{\text{fiber}}$  is the refractive index of the constituent material for the nanofiber [e.g., if  $\text{Si}_3\text{N}_4$  is adopted in Fig. 1(a),  $n_{\text{fiber}} = n_{\text{Si}_3\text{N}_4}$ ]. Then from the phase matching condition at the end-facet of nanofibers, these high- $k$  hyperbolic modes now have the chance to couple into the guided modes of the nanofiber. In contrast, most high- $k$  hyperbolic modes in Fig. 1(b) have  $|\text{Re}(k_x/k_0)| > n_{\text{fiber}}$ . They are thus intrinsically confined within the un-tilted metamaterials and cannot couple into the nanofiber.

Second, the reflection of hyperbolic modes, including those high- $k$  modes, at the end-facet of the nanofiber will be completely suppressed. This is because for a determined  $k_x$  in Fig. 1(c), there is only one hyperbolic mode, which corresponds to the incident hyperbolic mode, supported by the metamaterial. In other words, there will be no reflected propagating hyperbolic mode, since the reflected fields are evanescent with respect to the interface. This unavoidably leads to a high transformation of arbitrary incident hyperbolic modes in the colored region of Fig. 1(c) into the guided modes of nanofibers. In contrast, for the un-tilted hyperbolic metamaterials in Fig. 1(b), due to the existence of reflected propagating hyperbolic modes, the reflection of an incident hyperbolic mode (including the low- $k$  ones) cannot be avoided and is significant for high- $k$  modes.

From the above analyses, it is then straightforward to use the emerging unique feature of tilted hyperbolic metamaterials in Fig. 1(c) to enhance the on-chip photon extraction decay rate. This can be done, for example, simply by positioning a quantum emitter very close to a thin slab of the hyperbolic metamaterial, which is integrated with a nanofiber [Fig. 1(a)]. Here we focus on the weak coupling regime, and the quantum emitter is modeled by a dipole source<sup>8,29,48</sup> (see the supplementary material). Since the hyperbolic metamaterial has a broadband, extremely large photonic density-of-states,<sup>37–43</sup> the emitter has a large spontaneous emission rate  $\gamma_{\text{total}}$  or a large Purcell enhancement  $\gamma_{\text{total}}/\gamma_0$  (e.g.,  $>10^5$  in Fig. S4; see the supplementary material), where  $\gamma_0$  is the spontaneous emission rate of the quantum emitter in free space.

If the material loss is neglected, the on-chip photon extraction decay rate  $\gamma_{\text{fiber}}$  at a specific wavelength in Fig. 1(a) can be extremely large, and in principle, it can reach a value having the same order of magnitude as  $\gamma_{\text{total}}$  (i.e.,  $\gamma_{\text{fiber}} \sim \gamma_{\text{total}}$ ). This is enabled by the revealed capability of tilted hyperbolic metamaterials to efficiently transform the excited hyperbolic modes in the colored region of Fig. 1(c) into the guided modes of the nanofibers. It is then reasonable to expect  $\gamma_{\text{fiber}}$  to be quite large (e.g.,  $\gamma_{\text{fiber}}/\gamma_0 > 10^5$ ) in a broad spectral range, if the tilted hyperbolic metamaterial is transparent.

However, the material loss is unavoidable in practical passive hyperbolic metamaterials. We note that the realistic material loss can lead to a large reduction of  $\gamma_{\text{fiber}}$ , since the energy of excited high- $k$  modes will be largely degraded before they arrive at the end-facet of nanofibers. We then proceed to the study of  $\gamma_{\text{fiber}}$  in Figs. 2 and 3, with the consideration of realistic material losses in tilted hyperbolic metamaterials. Figures 2 and 3 show that we can still achieve  $\gamma_{\text{fiber}} \gg \gamma_0$  (e.g.,  $\gamma_{\text{fiber}} > 100\gamma_0$ ) over a broad spectral range, although we generally have  $\gamma_{\text{fiber}} \ll \gamma_{\text{total}}$ , instead of  $\gamma_{\text{fiber}} \sim \gamma_{\text{total}}$ , for realistic cases (see Fig. S4 in the supplementary material).

We begin our numerical study of  $\gamma_{\text{fiber}}$  at a specific wavelength in Fig. 2 (see the computation detail of  $\gamma_{\text{fiber}}$  in the supplementary material). For hyperbolic metamaterials, they are effectively constructed through alternating layers of metals and dielectrics. As a conceptual demonstration, the experimental data of permittivity of silver and silica<sup>49</sup> are adopted, and the metallic filling fraction is 50% (see the detailed strategy of structural design in the supplementary material). Due to the dispersion of constituent materials (e.g., metal), the critical angle  $\varphi_c(\lambda)$  of the designed hyperbolic metamaterial is sensitive to the wavelength [Fig. 2(a)].

Figure 2(b) shows  $\gamma_{\text{fiber}}$  as a function of the tilted angle  $\theta$ . The working wavelength (in free space) of  $\lambda_1 = 685$  nm is chosen for illustration, since it is within the radiation spectrum in which many of the currently considered quantum emitters operate, such as the range of 575–785 nm for the nitrogen-vacancy (NV) center in nano-diamonds.<sup>50</sup> The maximal  $\gamma_{\text{fiber}} \approx 460\gamma_0$  appears for the quantum emitter oriented along the  $z$  direction if  $\theta = \varphi_c(\lambda_1)$  in Fig. 2(b), where we have  $\varphi_c(\lambda_1) = 36^\circ$  from Fig. 2(a). Correspondingly, if  $\theta = \varphi_c(\lambda_1)$ , we find significant radiation fields being extracted into the nanofiber at  $\lambda_1$  in Fig. 2(c). As complementary information,  $\gamma_{\text{fiber}}$  is also studied for the quantum emitter oriented along the  $x$  or  $y$  direction in Fig. S4 (see the supplementary material). Importantly, the large value of  $\gamma_{\text{fiber}} > 400\gamma_0$  is always achievable if  $\theta = \varphi_c(\lambda_1)$ , independent of the orientation of quantum emitters. From Fig. 2 and Fig. S4, it is reasonable to argue that the proposed strategy to enhance  $\gamma_{\text{fiber}}$  via tilted (transparent) hyperbolic metamaterials in Fig. 1 works well for scenarios with reasonable amounts of loss.

Moreover, the proposed strategy in Fig. 1 is also applicable for the realistic lossy case over a broad spectral range, as shown in Fig. 3. To illustrate this point, Fig. 3 shows  $\gamma_{\text{fiber}}$  as a function of the wavelength ( $\lambda \in [575, 785]$  nm) and the tilted angle  $\theta$ . If  $\theta = \varphi_c(\lambda_1)$ ,  $\gamma_{\text{fiber}} > 100\gamma_0$  can be achieved over a continuous wavelength range with a bandwidth of  $\sim 80$  nm (Fig. 3). Note that the relative bandwidth, namely the bandwidth normalized by the central working wavelength, reaches  $12\% = \frac{80 \text{ nm}}{\lambda_1}$ .

On the other hand, it is noted that the feature of  $\gamma_{\text{fiber}}$  as a function of wavelength at  $\theta = \varphi_c(\lambda_1) \pm 1^\circ$  is similar to that at  $\theta = \varphi_c(\lambda_1)$  in Fig. 3. Such a phenomenon indicates that, due to materials losses,

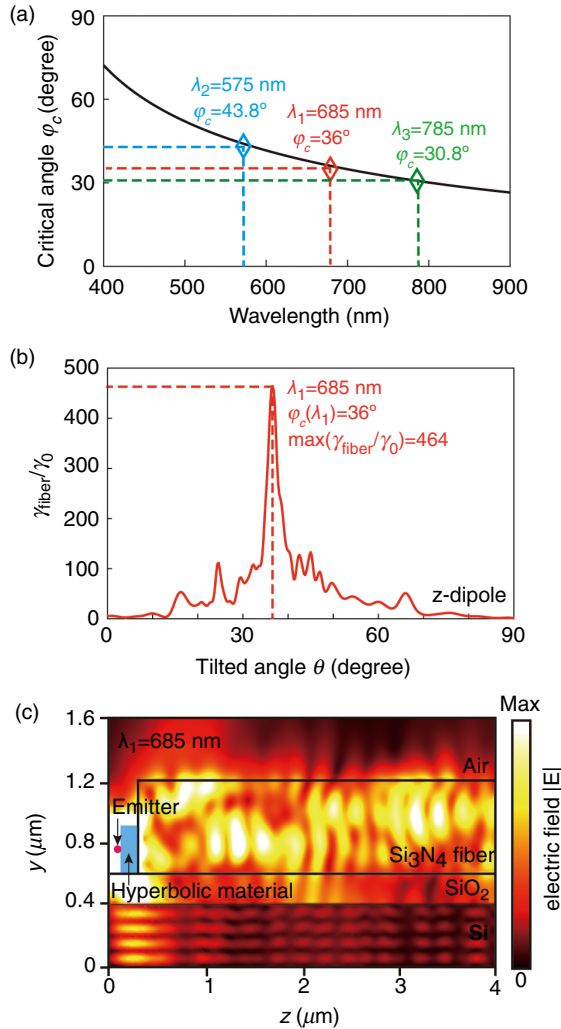


**FIG. 2.** Numerical demonstration of the enhancement of on-chip single-photon extraction via tilted hyperbolic metamaterials with realistic material losses. (a) Dependence of  $\varphi_c$  on the wavelength. This figure as well as Fig. 3 show that we can still achieve  $\gamma_{\text{fiber}} \gg \gamma_0$  (e.g.,  $\gamma_{\text{fiber}} > 100\gamma_0$ ) over a broad spectral range, although we generally have  $\gamma_{\text{fiber}} \ll \gamma_{\text{total}}$ , instead of  $\gamma_{\text{fiber}} \sim \gamma_{\text{total}}$ , for realistic cases (also see Fig. S4). (b) Normalized photon extraction rate  $\gamma_{\text{fiber}}/\gamma_0$  of a single emitter into the nanofiber as a function of the tilted angle  $\theta$ .  $\gamma_0$  is the spontaneous emission rate of a quantum emitter in free space. The working wavelength (in free space) of  $\lambda_1 = 685$  nm is chosen for illustration, since it is within the radiation spectrum in which many of the currently considered quantum emitters operate, such as the range of 575 to 785 nm for the NV center in nano-diamonds.<sup>50</sup> The maximal  $\gamma_{\text{fiber}} \approx 460\gamma_0$  appears for the quantum emitter oriented along the z direction if  $\theta = \varphi_c(\lambda_1)$  in Fig. 2(b), where we have  $\varphi_c(\lambda_1) = 36^\circ$  from Fig. 2(a). Correspondingly, if  $\theta = \varphi_c(\lambda_1)$ , we find significant radiation fields being extracted into the nanofiber at  $\lambda_1$  in Fig. 2(c). As complementary information,  $\gamma_{\text{fiber}}$  is also studied for the quantum emitter oriented along the x or y direction in Fig. S4. Importantly, the large value of  $\gamma_{\text{fiber}} > 400\gamma_0$  is always achievable if  $\theta = \varphi_c(\lambda_1)$ , independent of the orientation of quantum emitters. From Fig. 2 and Fig. S4, it is reasonable to argue that the proposed strategy to enhance  $\gamma_{\text{fiber}}$  via tilted (transparent) hyperbolic metamaterials in Fig. 1 works well for scenarios with reasonable amounts of loss. (c) Excited field distribution of a dipole-like emitter oriented along z direction, where  $\theta = \varphi_c(\lambda_1) = 36^\circ$ . The metamaterial and nanofiber have a cross-section of  $600 \times 300 \text{ nm}^2$  and  $600 \times 600 \text{ nm}^2$  in the xy plane, respectively. The metamaterial ( $\text{SiO}_2$  film) has a thickness of 200 nm in the z direction (200 nm in the y direction).  $\epsilon_{\text{Si}_3\text{N}_4} = n_{\text{Si}_3\text{N}_4}^2 = 4.37$  at 685 nm. The other structural setup is the same as in Fig. 1(c).

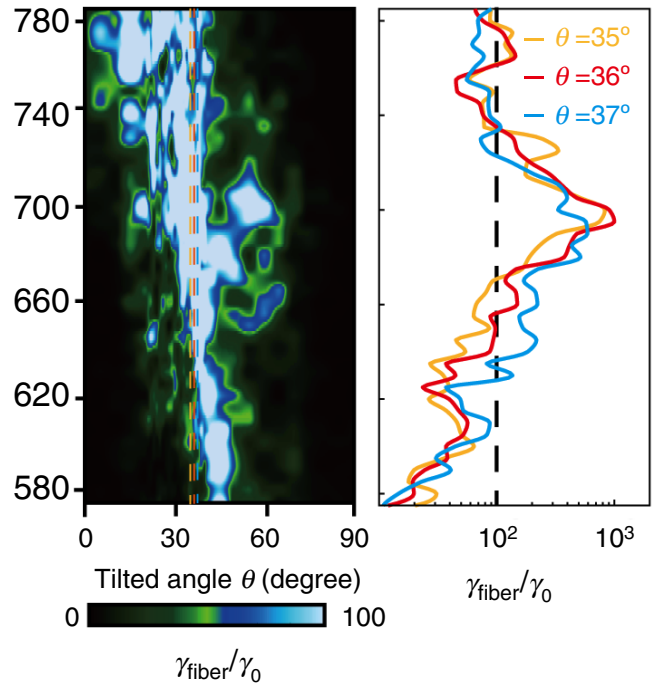


**FIG. 3.** Broadband enhancement of the on-chip single-photon extraction via tilted hyperbolic metamaterials. The left panel shows the normalized on-chip photon extraction rates  $\gamma_{\text{fiber}}/\gamma_0$  as a function of wavelength and the tilted angle  $\theta$ . In particular,  $\gamma_{\text{fiber}}/\gamma_0$  at  $\theta = \varphi_c(\lambda_1)$  and  $\varphi_c(\lambda_1) \pm 1^\circ$  are highlighted as a function of wavelength in the right panel, where  $\varphi_c(\lambda_1) = 36^\circ$ . The bandwidth of  $\gamma_{\text{fiber}}/\gamma_0 \geq 100$  can reach  $\sim 80$  nm for visible light if  $\theta \rightarrow \varphi_c(\lambda_1)$ . The basic setup is the same as Fig. 1(c). Here, due to materials losses, the hyperbolic mode with a finite large  $k$  ( $\leq k_{\text{max}}$ ), instead of the one with extremely large  $k$  ( $> k_{\text{max}}$ ), mainly contributes to the enhancement of  $\gamma_{\text{fiber}}$ .

the hyperbolic mode with a finite large  $k$  ( $\leq k_{\text{max}}$ ), instead of the one with extremely large  $k$  ( $> k_{\text{max}}$ ), mainly contributes to the enhancement of  $\gamma_{\text{fiber}}$ . This way, the requirement of  $\theta = \varphi_c(\lambda_1)$  in Fig. 1(c), which is applied to achieve large  $\gamma_{\text{fiber}}$  over a broad spectral range around  $\lambda_1$ , is not stringent for the realistic lossy case in Fig. 3. In other words, there is a certain tolerance on the choice of the tilted angle for the lossy cases. Such a loose requirement on the tilted angle in Fig. 3 may facilitate the practical implementation of the proposed structure in Fig. 1.

Last but not least, the permittivity of hyperbolic metamaterials can be described by the effective medium theory in an approximate way<sup>51–53</sup> or by the Bloch theorem in an accurate way with the consideration of their spatial dispersion.<sup>54,55</sup> Since  $\gamma_{\text{fiber}}$  for the realistic lossy cases is mainly related to the excited hyperbolic modes with  $k \leq k_{\text{max}}$ , it is reasonable and convenient to apply the effective medium theory in Figs. 2 and 3. To theoretically confirm this, for hyperbolic metamaterials, Fig. S5 (see the supplementary material) discusses the influence of their realistic structures or their spatial dispersion on  $\gamma_{\text{fiber}}$ ; to be specific, such an influence would be effectively suppressed if the periodicity of layered hyperbolic metamaterials is small enough. In addition, we show in Table I the direct comparison of photon extraction decay rate into free space or into nanofibers by using hyperbolic metamaterials between previous studies and this work. From Table I, it is

TABLE I. Comparison of photon extraction decay rates by using hyperbolic metamaterials.

Proposed structures (year published)	Photon extraction decay rate into air $\gamma_{\text{air}}$ or nanofiber $\gamma_{\text{fiber}}$
Layered (un-tilted and un-patterned) hyperbolic metamaterials (2015) <sup>29</sup>	$\gamma_{\text{air}}/\gamma_0 < 10$ , if $\lambda \in [600\ 800]$ nm
Nanopatterned (1D grating) hyperbolic metamaterials (2014) <sup>31</sup>	$10 < \gamma_{\text{air}}/\gamma_0 < 100$ , if $\lambda \in [500\ 650]$ nm
Nanopatterned (bullseye grating) hyperbolic metamaterials (2015) <sup>32</sup>	$10 < \gamma_{\text{air}}/\gamma_0 < 100$ , if $\lambda \in [600\ 700]$ nm
Photonic hypercrystals (2017) <sup>30</sup>	$100 < \gamma_{\text{air}}/\gamma_0 < 200$ , if $\lambda \in [580\ 700]$ nm
Adiabatically tapered hyperbolic metamaterials (2014) <sup>33</sup>	$\gamma_{\text{air}}/\gamma_0 < 100$ at $\lambda = 476$ nm
Un-tilted hyperbolic metamaterials integrated with nanofibers [this work]	$\gamma_{\text{fiber}}/\gamma_0 < 10$ , if $\lambda \in [575\ 785]$ nm
Tilted hyperbolic metamaterials integrated with nanofibers [this work]	$100 < \gamma_{\text{fiber}}/\gamma_0 < 1000$ , if $\lambda \in [660\ 740]$ nm

reasonable to argue that tilted hyperbolic metamaterials can be a promising platform for the enhancement of the on-chip photon extraction decay rate of quantum emitters over a broad spectral range.

In summary, we have proposed a simple yet universal scheme to enhance  $\gamma_{\text{fiber}}$  in a broad spectral range (e.g., a bandwidth of  $\sim 80$  nm in the visible regime) via tilted hyperbolic metamaterials. For tilted hyperbolic metamaterials, we let the tilted angle  $\theta$  of their optical axis be equal to their critical angle  $\varphi_c$ . Such a judicious geometrical tilting gives rise to some unique features of the hyperbolic isofrequency contour; in particular, it allows the excited high- $k$  hyperbolic modes to efficiently couple into the guided modes of the nanofiber almost without reflection. Two further advantages of the proposed scheme are the loose requirement on the tilted angle and the orientation of quantum emitters, which may facilitate its practical implementation. Our work also triggers many interesting open questions. As a prototypical example, if a quantum emitter is positioned close to a realistic hyperbolic metamaterial, the possibility to realize  $\gamma_{\text{fiber}}$  with its value in the same order of magnitude as  $\gamma_{\text{total}}$ , namely, the simultaneous realization of an extremely large spontaneous emission rate and a high coupling efficiency via hyperbolic metamaterials, still remains elusive.

### SUPPLEMENTARY MATERIAL

The [supplementary material](#) contains 6 sections, including critical angle  $\varphi_c$  of hyperbolic isofrequency contours, numerical computation details for  $\gamma_{\text{total}}$  and  $\gamma_{\text{fiber}}$ , structural design of hyperbolic metamaterials and effective medium theory, dependence of  $\gamma_{\text{total}}$  and  $\gamma_{\text{fiber}}$  on the orientation of quantum emitters, effective permittivity of hyperbolic metamaterials via Bloch theorem, and more discussion on  $\gamma_{\text{total}}$ .

### AUTHOR'S CONTRIBUTIONS

L.S. and X.L. contributed equally to this work.

### DATA AVAILABILITY

The data that supports the findings of this study are available within the article [and its [supplementary material](#)].

### ACKNOWLEDGMENTS

The work was sponsored by the National Natural Science Foundation of China (NNSFC) under Grant Nos. 61625502, 11961141010, 61975176, and 61905216; the Top-Notch Young Talents Program of China, and the Fundamental Research Funds for the Central Universities; the China Postdoctoral Science

Foundation (2018M632462); the Nanyang Technological University for NAP Start-Up Grant; and the Singapore Ministry of Education [Grant Nos. MOE2018-T2-1-022 (S), MOE2016-T3-1-006, and Tier 1 RG174/16 (S)].

### REFERENCES

- N. Gisin, G. Ribordy, W. Tittel, and H. Zbinden, *Rev. Mod. Phys.* **74**, 145 (2002).
- E. Knill, R. Laflamme, and G. J. Milburn, *Nature* **409**, 46 (2001).
- P. Kok, W. J. Munro, K. Nemoto, T. C. Ralph, J. P. Dowling, and G. J. Milburn, *Rev. Mod. Phys.* **79**, 135 (2007).
- T. E. Northup and R. Blatt, *Nat. Photonics* **8**, 356 (2014).
- M. R. Sprague, P. S. Michelberger, T. F. M. Champion, D. G. England, J. Nunn, X.-M. Jin, W. S. Kolthammer, A. Abdolvand, P. S. J. Russell, and I. A. Walmsley, *Nat. Photonics* **8**, 287 (2014).
- H. J. Kimble, *Nature* **453**, 1023 (2008).
- S. Slussarenko and G. J. Pryde, *Appl. Phys. Rev.* **6**, 041303 (2019).
- J. O'Brien, A. Furusawa, and J. Vuckovic, *Nat. Photonics* **3**, 687 (2009).
- P. Neumann, J. Beck, M. Steiner, F. Rempp, H. Fedder, P. R. Hemmer, J. Wrachtrup, and F. Jelezko, *Science* **329**, 542 (2010).
- M. V. Gurudev Dutt, L. Childress, L. Jiang, E. Togan, J. Maze, F. Jelezko, A. S. Zibrov, P. R. Hemmer, and M. D. Lukin, *Science* **316**, 1312 (2007).
- T. Schroder, F. Gadeke, M. J. Banholzer, and O. Benson, *New J. Phys.* **13**, 055017 (2011).
- E. Yablonovitch, *Phys. Rev. Lett.* **58**, 2059 (1987).
- M. D. Leistikov, A. P. Mosk, E. Yeganegi, S. R. Huisman, A. Lagendijk, and W. L. Vos, *Phys. Rev. Lett.* **107**, 193903 (2011).
- K. J. Russell, T.-L. Liu, S. Cui, and E. L. Hu, *Nat. Photonics* **6**, 459 (2012).
- A. V. Akimov, A. Mukherjee, C. L. Yu, D. E. Chang, A. S. Zibrov, P. R. Hemmer, H. Park, and M. D. Lukin, *Nature* **450**, 402 (2007).
- T. Kosako, Y. Kadoya, and H. F. Hofmann, *Nat. Photonics* **4**, 312 (2010).
- A. G. Curto, G. Volpe, T. H. Taminiau, M. P. Kreuzer, R. Quidant, and N. F. van Hulst, *Science* **329**, 930 (2010).
- X.-W. Chen, M. Agio, and V. Sandoghdar, *Phys. Rev. Lett.* **108**, 233001 (2012).
- C. Belacel, B. Habert, F. Bigourdan, F. Marquier, J.-P. Hugonin, S. Michaelis de Vasconcellos, X. Lafosse, L. Coolen, C. Schwob, C. Javaux, B. Dubretret, J.-J. Greffet, P. Senellart, and A. Maitre, *Nano Lett.* **13**, 1516 (2013).
- G. M. Akselrod, C. Argyropoulos, T. B. Hoang, C. Ciraci, C. Fang, J. Huang, D. R. Smith, and M. H. Mikkelsen, *Nat. Photonics* **8**, 835 (2014).
- Y. Chen, T. R. Nielsen, N. Gregersen, P. Lodahl, and J. Mørk, *Phys. Rev. B* **81**, 125431 (2010).
- J. Bleuse, J. Claudon, M. Creasey, N. S. Malik, J.-M. Gérard, I. Maksymov, J.-P. Hugonin, and P. Lalanne, *Phys. Rev. Lett.* **106**, 103601 (2011).
- Y. C. Jun, R. D. Kekatpure, J. S. White, and M. L. Brongersma, *Phys. Rev. B* **78**, 153111 (2008).
- V. V. Klimov and M. Ducloy, *Phys. Rev. A* **69**, 013812 (2004).
- R. Yalla, F. Le Kien, M. Morinaga, and K. Hakuta, *Phys. Rev. Lett.* **109**, 063602 (2012).
- L. Liebermeister, F. Petersen, A. V. Munchow, D. Burchardt, J. Hermelbracht, T. Tashima, A. W. Schell, O. Benson, T. Meinhardt, A. Krueger, A. Stiebeiner,

- A. Rauschenbeutel, H. Weinfurter, and M. Weber, *Appl. Phys. Lett.* **104**, 031101 (2014).
- <sup>27</sup>R. N. Patel, T. Schroder, N. Wan, L. Li, S. L. Mouradian, E. H. Chen, and D. R. Englund, *Light Sci. Appl.* **5**, e16032 (2016).
- <sup>28</sup>H. Lian, Y. Gu, J. Ren, F. Zhang, L. Wang, and Q. Gong, *Phys. Rev. Lett.* **114**, 193002 (2015).
- <sup>29</sup>M. Y. Shalaginov, V. V. Vorobyov, J. Liu, M. Ferrera, A. V. Akimov, A. Lagutchev, A. N. Smolyaninov, V. V. Klimov, J. Irudayaraj, A. V. Kildishev, A. Boltasseva, and V. M. Shalae, *Laser Photonics Rev.* **9**, 120 (2015).
- <sup>30</sup>T. Galfsky, J. Gu, E. E. Narimanov, and V. M. Menon, *PNAS* **114**, 5125–5129 (2017).
- <sup>31</sup>D. Lu, J. J. Kan, E. E. Fullerton, and Z. Liu, *Nat. Nanotechnol.* **9**, 48 (2014).
- <sup>32</sup>T. Galfsky, H. N. S. Krishnamoorthy, W. Newman, E. E. Narimanov, Z. Jacob, and V. M. Menon, *Optica* **2**, 62 (2015).
- <sup>33</sup>P. R. West, N. Kinsey, M. Ferrera, A. V. Kildishev, V. M. Shalae, and A. Boltasseva, *Nano Lett.* **15**, 498 (2015).
- <sup>34</sup>L. Ferrari, J. S. T. Smalley, Y. Fainman, and Z. Liu, *Nanoscale* **9**, 9034 (2017).
- <sup>35</sup>E. Bermúdez-Ureña, C. Gonzalez-Ballester, M. Geiselmann, R. Marty, I. P. Radko, T. Holmgaard, Y. Alaverdyan, E. Moreno, F. J. García-Vidal, S. I. Bozhevolnyi, and R. Quidant, *Nat. Commun.* **6**, 7883 (2015).
- <sup>36</sup>S. L. Mouradian, T. Schröder, C. B. Poitras, L. Li, J. Goldstein, E. H. Chen, M. Walsh, J. Cardenas, M. L. Markham, D. J. Twitchen, M. Lipson, and D. Englund, *Phys. Rev. X* **5**, 031009 (2015).
- <sup>37</sup>P. Huo, S. Zhang, Y. Liang, Y. Lu, and T. Xu, *Adv. Opt. Mater.* **7**, 1801616 (2019).
- <sup>38</sup>A. Poddubny, I. Iorsh, P. Belov, and Y. Kivshar, *Nat. Photonics* **7**, 948 (2013).
- <sup>39</sup>P. Shekhar, J. Atkinson, and Z. Jacob, *Nano Convergence* **1**, 14 (2014).
- <sup>40</sup>L. Ferrari, C. Wu, D. Lepage, X. Zhang, and Z. Liu, *Prog. Quantum Electron.* **40**, 1 (2015).
- <sup>41</sup>Z. Jacob, J. Kim, G. V. Naik, A. Boltasseva, E. E. Narimanov, and V. M. Shalae, *Appl. Phys. B: Lasers Opt.* **100**, 215 (2010).
- <sup>42</sup>Z. Jacob, I. I. Smolyaninov, and E. E. Narimanov, *Appl. Phys. Lett.* **100**, 181105 (2012).
- <sup>43</sup>H. N. Krishnamoorthy, Z. Jacob, E. Narimanov, I. Kretschmar, and V. M. Menon, *Science* **336**, 205 (2012).
- <sup>44</sup>J. D. Caldwell, A. V. Kretinin, Y. Chen, V. Giannini, M. M. Fogler, Y. Francescato, C. T. Ellis, J. G. Tischler, C. R. Woods, A. J. Giles, M. Hong, K. Watanabe, T. Taniguchi, S. A. Maier, and K. S. Novoselov, *Nat. Commun.* **5**, 5221 (2014).
- <sup>45</sup>A. J. Giles, S. Dai, O. J. Glembocki, A. V. Kretinin, Z. Sun, C. T. Ellis, J. G. Tischler, T. Taniguchi, K. Watanabe, M. M. Fogler, K. S. Novoselov, D. N. Basov, and J. D. Caldwell, *Nano Lett.* **16**, 3858 (2016).
- <sup>46</sup>L. V. Brown, M. Davanco, Z. Sun, A. Kretinin, Y. Chen, J. R. Matson, I. Vurgaftman, N. Sharac, A. J. Giles, M. M. Fogler, T. Taniguchi, K. Watanabe, K. S. Novoselov, S. A. Maier, A. Centrone, and J. D. Caldwell, *Nano Lett.* **18**, 1628 (2018).
- <sup>47</sup>X. Wu, C. A. McEleney, M. González-Jiménez, and R. Macêdo, *Optica* **6**, 1478 (2019).
- <sup>48</sup>M. S. Yeung and T. K. Gustafson, *Phys. Rev. A* **54**(6), 5227 (1996).
- <sup>49</sup>P. B. Johnson and R. W. Christy, *Phys. Rev. B* **6**, 4370 (1972).
- <sup>50</sup>M. W. Doherty, N. B. Manson, P. Delandy, F. Jelezko, J. Wrachtrup, and L. C. L. Hollenberg, *Phys. Rep.* **528**(1), 1 (2013).
- <sup>51</sup>L. D. Landau and E. M. Lifshitz, *Course of Theoretical Physics* (Pergamon Press, Oxford, 1959).
- <sup>52</sup>L. Brekhovskikh, *Waves in Layered Media* (Elsevier, New York, 2012).
- <sup>53</sup>L. Shen, L. Prokopenko, H. Chen, and A. Kildishev, *Nanophotonics* **7**, 479 (2017).
- <sup>54</sup>P. Yeh, A. Yariv, and C.-S. Hong, *J. Opt. Soc. Am.* **67**, 423 (1977).
- <sup>55</sup>H. Hu, X. Lin, J. Zhang, D. Liu, P. Genevet, B. Zhang, and Y. Luo, *arXiv:2002.04252* (2020).